J Mol Model (2009) 15:461–468
DOI 10.1007/s00894-008-0427-4

ORIGINAL PAPER

Density functional studies of closed-shell attractions of $S(AuPH_3)_2$ and $HS(AuPH_3)_2^+$ and their dimers

Hua Fang · Xiao-Gang Zhang · Shu-Guang Wang

Received: 4 September 2008 / Accepted: 17 November 2008 / Published online: 13 December 2008

Abstract With the help of quantum chemical calculations, $S(AuPH_3)_2$, $[HS(AuPH_3)_2]^+$ and their dimers have been examined by using scalar-relativistic theory. In agreement with experimental data, $[HS(AuPH_3)_2^+]_2$ is a C_{2h} structure. However, $[S(AuPH_3)_2]_2$ is predicted to favor a D_{2d} structure. Experimental structure parameters of the title compounds were reproduced at the Xα level. The electronic structure and HOMO–LUMO gaps were investigated. When two monomers formed a dimer, the electronic structure of the dimer changed only slightly, but the chemical stability decreased. The intermolecular aurophilic interaction energy is decomposed and analyzed.

Keywords Aurophilic interaction · Bond energy decomposition · Closed-shell · Density functional · Electronic structure · Mulliken population

Introduction

The chemistry of gold has undergone a fascinating and almost explosive development, which is related to the discovery of novel compounds exhibiting unusual structures. The structural chemistry of Au(I) complexes shows many examples of inter- and intra-molecular contacts of about 3 Å between the closed-shell (d^{10}) metal centers. This phenomenon is strengthened by relativistic effects [1].

The stabilization of molecular systems associated with this type of bonding is particularly strong in polynuclear species, where gold atoms can cluster in small aggregates, either in a homo- or hetero-atomic way [2, 3]. Element-centered Au(I) clusters of hypercoordinate carbon, nitrogen, and phosphorus are among the most striking examples of this new type of aggregation [4–7]. For sulfur, the chemistry of Au(I) clusters of this type was originally [8–10] limited to trigoldsulfonium cations of the type $[S(AuL)_3]^+$; subsequently, this class of compounds was also extended [11]. Similar structural motifs can be found in a large number of recently synthesized gold complexes [12–18].

Some central-atom Au(I) complexes are grouped in pairs through inter-molecular Au(I)···Au(I) contacts [9, 19, 20]. It has been reported that, in the solid state $[R'S(AuPR_3)_2]^+$ are found as dimers [21–23] by loosely associating through parallel edge–edge contacts with Au···Au distances of about 3.10 Å. For aurophilic interaction systems, where dispersion interaction plays an important role, it was thought that density functional (DF) methods are not applicable. However, there is now much evidence that a careful choice of the DF gives reasonable bond lengths and bond energies of Au(I) cluster systems [24–27].

In the present work we report a theoretical study of several gold–thiolate complexes $S(AuPH_3)_2$, $[HS(AuPH_3)_2]^+$ and the dimer of $[HS(AuPH_3)_2]^+$, which serve as models of the synthesized compounds $S(AuL)_2$ [17], $[MeS(AuPMe_3)_2^+]_2$ (Me=methyl) [28] and $[RS(AuL)_2]_2^{2+}$ [21–23]. The calculated geometries are compared with

H. Fang (✉) · X.-G. Zhang
College of Material Science & Technology,
Nanjing University of Aeronautics and Astronautics,
Nanjing 210016, PR China
e-mail: susanfang@nuaa.edu.cn

S.-G. Wang
School of Chemistry and Chemical Technology,
Shanghai Jiao Tong University,
Shanghai 200240, PR China

available crystallographic data, and the electronic structure and intermolecular bonding of these complexes are analyzed. At the same time, the geometry of $S(AuPH_3)_2$ dimers is predicted. Therefore, our study will also shed some light on how crystal packing and dimerization affect the geometries of these complexes.

Methods

Models

Models of the experimental structures $RS(AuPPh_3)_2^+$ and the dimer of $RS(AuPPh_3)_2^+$ (R=H or none) used in our study are shown in Fig. 1. In the experimental structures, the ligand is typically triphenylphosphine, $-P(C_6H_5)_3$. For computational efficiency, it was replaced by the unsubstituted phosphine group, $-PH_3$. This substitution has been found to have little influence on X–Au and Au–P bond lengths [29], while permitting the calculations of larger systems with reasonable computational effort.

Computational details

The geometries were fully optimized using MP2 and several DFT methods. The calculations were carried out with GAUSSIAN 98 [30] and the ADF 2004 package initially developed by Baerends et al. [31].

In addition, several different versions of the exchange-correlation DF were carried out to calculate the systems. We used: (1) the simple local Xα exchange potential [32–35], with parameter α=0.7; (2) the local correlation-corrected version developed by Vosko, Wilk and Nusair [36]; (3) the nonlocal gradient-corrected exchange potential of Becke [37] and the nonlocal gradient-corrected correlation potential of Perdew [38]; and (4) the generalized gradient approach of Perdew and Wang (PW91) [39].

High quality triple-ξ, Slater-type plus two polarization (TZ2P) orbital basis sets were used for the valence shells of all atoms. To reduce the number of electrons in the gold complexes, the inner core shells were frozen [40], namely [$1s^2$-$4f^{14}$] for Au, [$1s^2$-$2p^6$] for S and P. Relativistic effects are particularly important for gold and aurophilic interactions. We used the scalar relativistic zeroth order regular approximation (ZORA) [41–44], which averages over spin-orbit splittings. Spin-orbit effects are expected to be unimportant to Au(I) systems. For the dimer, fragment binding energies were calculated as differences between the total energies of the complex and the sum of the energies of its fragments.

The Gaussian basis sets were used for MP2 calculations: for gold, the 19 valence-electron (VE) of the Au quasi-relativistic (QR) pseudo-potential (PP) of Andrae et al. [45] was used. We added two f-type polarization functions on gold (α_f=0.2 and α_f=1.19) [46]. The S, P and H atoms used double-zeta basis sets.

Results and discussion

Structures of $S(AuPH_3)_2$ and $HS(AuPH_3)_2^+$

To analyze the geometric and electronic structures of the gold-thiolate compounds $[R'S(AuPR_3)_2]^+$ with larger ligands PR_3 and SR′, we carried out MP2 and DF calculations on the corresponding model complexes $S(AuPH_3)_2$ and $[HS(AuPH_3)_2]^+$. While several different species with one or two gold-phosphine groups ($AuPR_3$) are known, we report here the results of geometry optimizations of pertinent structural parameters of the systems. In the case of polynuclear complexes, we give the Au···Au distance and the Au–S–Au angle, since the Au···Au interaction may play a role in these systems [1, 2]. Other internal coordinates, although included in the optimization, will not be displayed here since they are less important for a discussion of the structures.

First, we compared the fully optimized structures of the monomer as obtained by means of MP2 and several DF methods, and by experiment. For the $S(AuPH_3)_2$ molecule, as shown in Table 1, the Hartree-Fock (HF) [47] method was unable to give reasonable results. With the correlation correction of MP2 [47], both calculated Au–S and Au–P bond lengths are in good agreement with experimental values. However, the Au···Au distance and the Au–S–Au bond angle are smaller than experimental values by 10 pm and 9°, respectively. Local DF VWN and Xα give similar results. The Au–P, Au–S bond lengths and Au–S–Au bond angle obtained by VWN and Xα methods were reproduced. The Au···Au distances are in agreement with experimental values at 2 pm. When nonlocal exchange and correlation correction are added (BP, PW91), the Au···Au distance determined by the BP method increases about 3 pm and the Au–S–Au angle obtained by BP decreases by 5°, while the results obtained with PW91 are even longer.

Recently, MP4 and CCSD(T) have been applied to a $S(AuPH_3)_2$ molecule [48]; deviations between theoretical and experimental data remained. Our Xα method gives even better results than CCSD(T). All calculated S–Au and Au–P distances are significantly larger than experimental distances. This may indicate that crystal structure effects play an important role.

For the $HS(AuPH_3)_2^+$ molecule, with the correlation correction of MP2, calculated Au–P bond lengths are in agreement with experimental values. Compared to experimental values, the Au–S bond length obtained by MP2 is

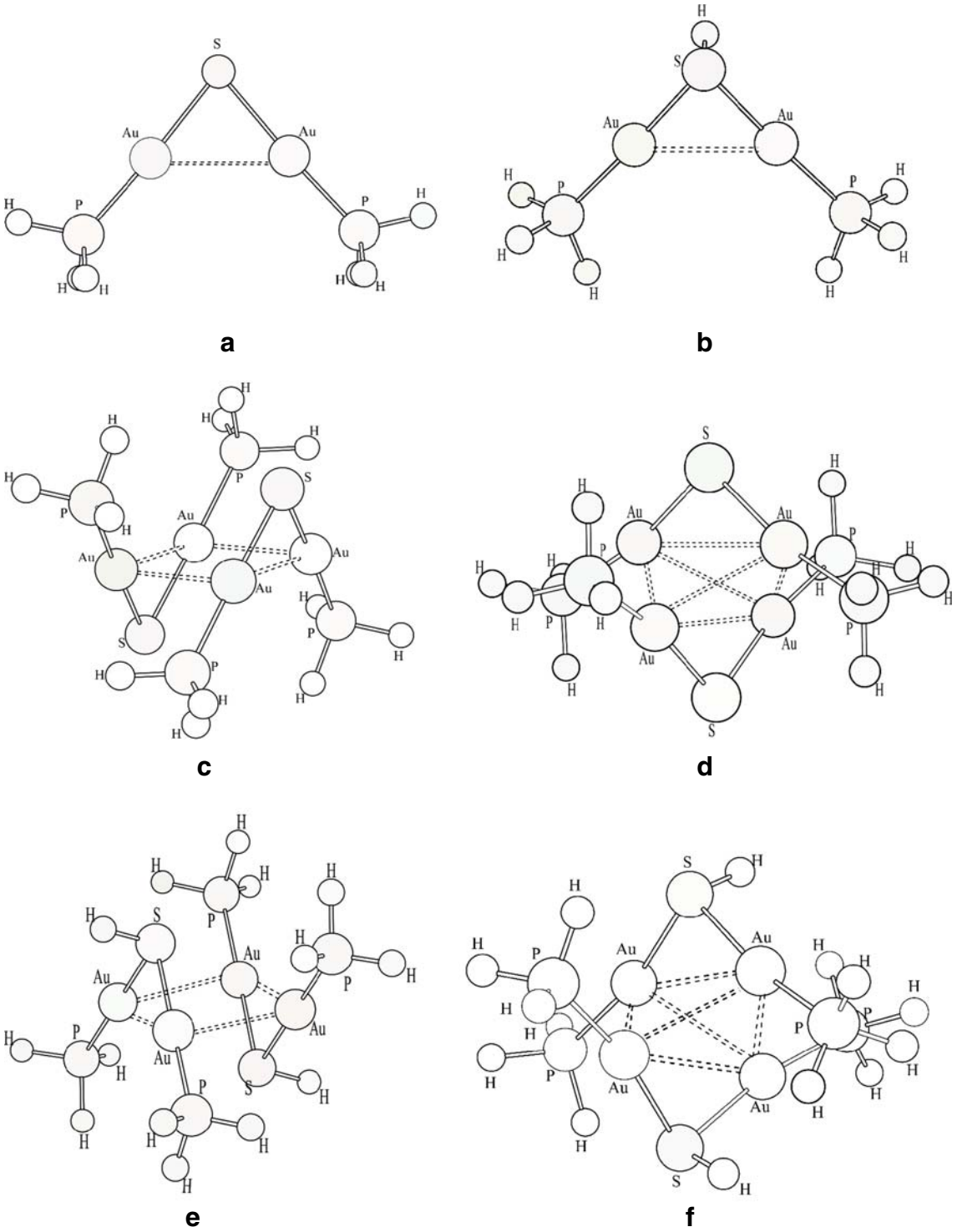

Fig. 1 Geometries of the systems studied. **a** $S(AuPH_3)_2$ (C_{2v}), **b** $HS(AuPH_3)_2^+$ (Nosym), **c** $[S(AuPH_3)_2]_2$ (C_{2h}), **d** $[S(AuPH_3)_2]_2$ (D_{2d}), **e** $[HS(AuPH_3)_2^+]_2$ (C_{2h}), **f** $[HS(AuPH_3)_2^+]_2$ (C_2)

underestimated by 4 pm, while the Au···Au distance is shorter than the experimental value by 20 pm. Local DFs (VWN, Xα) give similar results. Au–P, Au–S bond lengths obtained by VWN and Xα methods are reproduced. The Au···Au distances come to an agreement with the experimental values within 2–4 pm. When nonlocal exchange and correlation correction are added (BP, PW91), the Au···Au distance by BP and PW91 methods increase by more than 25 pm. The DF results compare reasonably well with the MP2 results.

Table 1 Main geometric parameters of $S(AuPH_3)_2$ and $HS(AuPH_3)_2^+$ (in pm and degrees)

System	Method	$R_{Au\cdots Au}$	R_{Au-S}	R_{Au-P}	$\theta_{Au-S-Au}$
$S(AuPH_3)_2$	HF[a]	356.3	233.6	236.9	99.4
	MP2[a]	291.1	228.2	227.3	79.3
	MP4[b]	292.1	230.6	230.3	78.6
	CCSD(T)[b]	303.0	231.3	232.1	81.8
	Xα	299.0	226.2	222.0	82.9
	VWN	298.0	225.5	221.0	82.7
	BP	305.0	229.3	225.0	83.5
	PW91	306.0	228.0	226.0	84.2
	Exp[c]	301.8	215.9	213.5	88.7
$HS(AuPH_3)_2^+$	MP2	282.3	231.0	225.0	74.6
	Xα	301.0	231.0	224.0	81.2
	VWN	299.0	230.9	224.0	81.0
	BP	355.0	235.4	227.0	98.2
	PW91	348.0	235.0	224.0	95.6
	LDA[d]	296.2	231.2	224.6	
	Exp[e]	303.3	235.2	224.1	
	Exp[f]	304-330	234.0	227.0	

[a] HF and MP2 results [47]
[b] MP4 and CCSD(T) results [48]
[c] Experimental values [17]
[d] LCGTO-DF results [49]
[e] Experimental values [28]
[f] Experimental values [21, 23, 50, 51]

For the two monomers $S(AuPH_3)_2$ and $HS(AuPH_3)_2^+$, Xα is the most suitable method. There is an obvious difference between the $S(AuPH_3)_2$ and $HS(AuPH_3)_2^+$ molecules. When the apical S atom obtained one additional H^+ proton, the Au···Au distance, Au–S and Au–P bond lengths increase by 2 pm, 5 pm and 2 pm, respectively. On the contrary, the Au–S–Au and S–Au–P angles reduce by not more than 2°.

Structures of $[S(AuPH_3)_2]_2$ and $[HS(AuPH_3)_2^+]_2$

$HS(AuPH_3)_2^+$ cation moieties tend to dimerize in the crystal, with interionic Au···Au separations slightly larger than 3 Å [21–23]; structure shown in Fig. 1e. The dimer of $HS(AuPH_3)_2^+$ was calculated by MP2 and several DF methods. The calculated structures of $HS(AuPH_3)_2^+$ dimers are displayed in Table 2. For the $[HS(AuPH_3)_2^+]_2$ molecule, both Au–S and Au–P bond lengths calculated by the MP2 and DF methods are consistent with experimental values. At the MP2 level, the inter- and intra- molecular Au···Au distances are shorter than experimental values by about 30 pm. Local density functionals (VWN, Xα) give similar results. Au–P and Au–S bond lengths obtained by VWN and Xα methods are reproduced. The intra-molecular Au···Au distance calculated by both VWN and Xα methods are similar to experiment values, while the inter-molecular Au···Au distance obtained by the VWN method is underestimated by 10 pm. The inter-molecular Au···Au distance obtained by the Xα method is similar to experimental values. When nonlocal exchange and correlation correction are added (BP, PW91), the intra- and inter-molecular Au···Au distances increase by about 30–50 pm.

Table 2 Main geometric parameters of $[HS(AuPH_3)_2^+]_2$

System	Method	$R_{Au\cdots Au}^{intra}$	$R_{Au\cdots Au}^{inter}$	R_{Au-S}	R_{Au-P}	$\theta_{Au-S-Au}$
$[HS(AuPH_3)_2^+]_2$	MP2	283.0	281.0	234.0	226.0	74.2
	Xα	317.0	308.0	232.9	226.0	85.9
	VWN	311.0	303.0	232.2	225.0	84.1
	BP	370.0	347.0	237.1	228.0	102.6
	PW91	367.0	330.0	235.0	228.0	102.8
	Exp [a]	310.0	313.0	235.4	227.5	

[a] Experimental values [23]

$[Cl(AuL)_2^+]_2$ has been reported experimentally [52] (its structure is similar to the structure shown in Fig. 1d). We calculated the C_{2h} $[HS(AuPH_3)_2^+]_2$ at the Xα level and the results are displayed in Table 3. At the same time, the C_{2h} and D_{2d} geometries of $[S(AuPH_3)_2]_2$ were also predicted theoretically at the Xα level.

We found that the energy of D_{2d} $[S(AuPH_3)_2]_2$ is 30.99 kJ/mol lower than that of the C_{2h} structure. That means $[S(AuPH_3)_2]_2$ prefers a D_{2d} structure. On the contrary, for $[HS(AuPH_3)_2^+]_2$ the energy of the C_{2h} structure is 7.78 kJ/mol lower than that of the C_2 structure. $[HS(AuPH_3)_2^+]_2$ prefers the C_{2h} structure, which is consistent with the experimental structure.

Comparing structural parameters of $S(AuPH_3)_2$, $HS(AuPH_3)_2^+$ to their dimers

For $S(AuPH_3)_2$ and $HS(AuPH_3)_2^+$ systems, the structural parameters obtained by the Xα method are closest to the experimental values. Obviously, when two monomers form a dimer, this association affects the structural parameters of the dimer. The change in Au···Au intra-distance, Au–P, Au–S bond lengths, and Au–S–Au and S–Au–P angles are shown in Table 4.

The intra-molecular Au···Au distance is initially 299 pm in $S(AuPH_3)_2$, and the Au–S–Au and S–Au–P angles are 82.9° and 178.7°, respectively. When two monomers form one dimer, the intra-molecular Au···Au distance is elongated by 17 pm, the Au–S–Au angle widens by 4° while the S–Au–P angle narrows by 4°, i.e., the deviation from linearity of

Table 3 Structural parameters for $[S(AuPH_3)_2]_2$ and $[HS(AuPH_3)_2^+]_2$ at Xα/TZ2P level. Bond distances in picometers, angles in degrees

System	Sym.	$R_{Au\cdots Au}^{intra}$	$R_{Au\cdots Au}^{inter}$	R_{Au-S}	R_{Au-P}	$\theta_{Au-S-Au}$
$[S(AuPH_3)_2]_2$	C_{2h}	287.0	301.0	229.0	223.0	77.5
	D_{2d}	315.7	298.0	229.0	225.0	87.0
$[HS(AuPH_3)_2^+]_2$	C_{2h}	317.0	308.0	232.9	226.0	85.9
	C_2	349.3	296.0	234.0	226.0	96.4

Table 4 Changes in bond lengths (pm) and bond angles (°) upon forming dimers

System	$R_{Au\cdots Au}^{intra}$	$R_{Au\cdots Au}^{inter}$	$R_{Au\text{-}S}$	$R_{Au\text{-}P}$	$\theta_{Au\text{-}S\text{-}Au}$	$\theta_{S\text{-}Au\text{-}P}$
$S(AuPH_3)_2$	299.0		226.2	222.0	82.9	178.7
$[S(AuPH_3)_2]_2$	315.7	298.0	229.0	225.0	87.0	174.7
$HS(AuPH_3)_2^+$	301.0		231.0	224.0	81.2	177.5
$[HS(AuPH_3)_2^+]_2$	317.0	308.0	232.9	226.0	85.9	179.3

the S–Au–P angle is greater after forming the dimer. This greater deviation from linearity means a bending of the S–Au–P axes, which brings the gold atoms closer together.

When two $HS(AuPH_3)_2^+$ molecules form $[HS(AuPH_3)_2^+]_2$, the intra-molecular Au···Au distance, Au–S and Au–P bond lengths are elongated by 16 pm, 2 pm and 2 pm, respectively. The Au–S–Au bond angle is widened by 5°. The S–Au–P angle in the monomer is 177.5°. The deviation from linearity is 2.5° in the monomer, while in the dimer the S–Au–P angle is 179.3°. Since the monomer forms the dimer through edge–edge Au···Au contacts, the influence of steric repulsion of the larger phosphine ligand on the structure of the dimer is small. The deviation from linearity is 0.7° in the dimer, i.e., smaller than the deviation in the monomer.

Mulliken populations and charges of $S(AuPH_3)_2$, $[HS(AuPH_3)_2]^+$ and their dimers

Thirdly, we will discuss the charge distribution by means of Mulliken population analysis. In Table 5, we can see that the effective Mulliken charges on the gold atoms of $S(AuPH_3)_2$, $[HS(AuPH_3)_2]^+$ and their dimers are about 0.1. At the same time, there are approximately 0.5 *e* electron holes in the Au5d shell, 1.0 *e* in the Au6s and 0.3 to 0.5 *e* in the Au6p valence shells. From the data, the PH_3 ligands transfer 0.1 to 0.5 electronic charges to the Au atom, so that the gold atoms effectively carry only very small positive charges. In these systems, there are almost 0.5±0.1 electron holes in the Au5d shell, and the ~1.0 *e* in the 6s and ~0.4 *e* in the 6p valence shells. The small effective charges on Au seem to enhance Au (I)···Au (I) attraction [24]. We did not know whether the stabilities were affected by effective charges on Au. Note that the effective charges in Table 5 are the gross values. The phosphine ligands, of course, decrease the effective atomic charge on the gold atom, Q_{Au}. At the same time, phosphine ligands increase the Mulliken charges of Au6p, Au5d, Au5f shells. Au (5d) and Au (6p) participation in gold cluster formation may be essential to explain the high stabilities in such systems.

The Au 5d orbital can make a definite, albeit small, contribution to the Au···Au bond. The radial bonds of the gold cluster (to the central sulfur atom as well as to the outer ligands) lead to a further reduction in the Au 5d population, thereby improving the possibility of an aurophilic interaction. We can see that the Mulliken populations and charges of the monomer are similar to those of the dimer. The interaction between the monomers is too small to noticeably change their electronic structure. Thus, no significant changes in the Mulliken populations and in the effective configuration of the Au atoms are induced by dimerization. These results show that the 5d shell is not completely closed, and thus it may contribute to metal–metal bonding.

Analyzing the HOMO–LUMO Gap

Next, the HOMO–LUMO energy gap for $S(AuPH_3)_2$, $[HS(AuPH_3)_2]^+$ and their dimers were analyzed using the Xα method; the results are shown in Table 6. The HOMO–LUMO gap of $S(AuPH_3)_2$ is 2.767 eV, and the gap of $HS(AuPH_3)_2^+$ is 4.616 eV. When the top S atom obtained one H^+ proton, the HOMO–LUMO gap increased by 1.849 eV. Comparing the HOMO–LUMO gap of $[HS(AuPH_3)_2]_2^{2+}$ to that of $[S(AuPH_3)_2]_2$, the gap increases by 1.581 eV. When $S(AuPH_3)_2$ and $HS(AuPH_3)_2^+$ formed dimers, the HOMO–LUMO gap decreased by about 0.4–0.7 eV, and the chemical stability decreased.

Bond energy decomposition

According to the theory of Ziegler [53], bond energy can be split into two parts [54, 55]. One is the "steric interaction energy" ($E_{ster.}$), which comes from the electrostatic interac-

Table 5 Mulliken populations and charges of $S(AuPH_3)_2$, $[HS(AuPH_3)_2]^+$ and their dimers at the Xα/TZ2P level

System	Sym.	Au6s	Au6p	Au5d	Au5f	Q_{Au}	Q_S	Q_{PH3}	Q_H[a]
$S(AuPH_3)_2$	C_{2v}	1.04	0.43	−0.56	0.03	0.06	−0.46	0.17	
$[HS(AuPH_3)_2]^+$	Nosym	1.03	0.35	−0.49	0.03	0.08	0.02	0.40	0.02
$[S(AuPH_3)_2]_2$	D_{2d}	1.01	0.53	−0.55	0.03	-0.02	−0.44	0.24	
$\{H[S(AuPH_3)_2]^+\}_2$	C_{2h}	1.01	0.41	−0.48	0.03	0.03	0.00	0.46	0.02

[a] Top H

Table 6 HOMO–LUMO gap $\Delta\varepsilon_i$ (in eV) of $S(AuPH_3)_2$, $[HS(AuPH_3)_2]^+$ and their dimers (at Xα/TZ2P level)

	$S(AuPH_3)_2$		$HS(AuPH_3)_2^+$		$[S(AuPH_3)_2]_2$		$[HS(AuPH_3)_2]_2^{2+}$	
	Orbital	Energy	Orbital	Energy	Orbital	Energy	Orbital	Energy
LUMO	12a1	−1.112	31a	−4.956	5b1	−1.549	17a.g	−7.602
HOMO	5b1	−3.879	30a	−9.572	15e1	−3.868	14b.g	−11.512
$\Delta\varepsilon_i$		2.767		4.616		2.319		3.910

tion ($E_{ele.}$) between the fragments (with unchanged electron densities) and the Pauli exchange repulsion (E_{pauli}) due to the antisymmetry requirement raising the energy when occupied fragment orbitals overlap. The other is the "orbital interaction energy" ($E_{orb.}$) due to quantum mechanical interference and orbital relaxation from the initial fragment states to the final molecular states. The orbital interaction contains charge transfer contributions (mixing of occupied orbitals on one fragment and virtual orbitals on the other fragment) and polarization contributions (mixing of occupied and virtual orbitals on the fragment itself). The bond energies are analyzed and presented in Table 7.

The calculated binding energies, $BE=E\{[RS(AuPH_3)_2^q]_2\}-2E\{[RS(AuPH_3)_2^q]\}$(R=H with q=+1and none with q=0), are displayed in Table 7; negative values of BE correspond to an exothermic reaction $2[RS(AuL)_2^q]\rightarrow[RS(AuL)_2^q]_2$. For the systems $[S(AuPH_3)_2]_2$, the intermolecular aurophilic interaction is 124.8 kJ/mol. The intermolecular energy of each Au···Au pair is about 31 kJ/mol, and in the range of aurophilic interaction [1]. Although the repulsion between the two unperturbed monomers amounts to 96.69 kJ/mol, the self-consistently relaxed dimer (with electron correlation at the Xα level of approximation) becomes bound, namely by −124.8 kJ/mol through an energy lowering of −221.49 kJ/mol, due to orbital mixing. That is, when the Au(I) closed shells approach each other, Pauli overlap repulsion increases comparatively slowly, whereas the electrostatic overlap attraction increases significantly enough that the combined effect of orbital mixing and electron correlation add up to a 'secondary bond'.

For the $[HS(AuPH_3)_2^+]_2$ system, a positive BE value (no bonding) was obtained. Obviously, this overall repulsive behavior is due to the Coulomb interaction between the charged monomer species. We know, however, that repulsions between ions of like charge expected for a dimer in the gas phase are attenuated in the solid state by the Madelung potential provided by the counterions. For such a system, in order to simulate in an approximate fashion the stabilization of the dications in the crystal environment, two point charge (PC) models were constructed to represent the Madelung field set up by the counterions.

For the $[HS(AuPH_3)_2^+]_2$ system, a potential curve to solve the effect of the counterions to the aurophilic interaction was plotted. The resulting values for the Xα level energy as a function of $R_{Au\text{-}Au'}$ is shown in Fig. 2 for relativistic calculations. The energy zero is taken as 2 $HS(AuPH_3)_2^+$ at infinite separation. In Fig. 2, the potential curve is shown in a large *R*-range. Inspection of Fig. 2 shows that the calculated values of the dimer binding energy depend considerably on the PC model chosen. For the $[HS(AuPH_3)_2^+]_2$ dimer, negative binding energies are obtained. In particular, there is a potential well about 334 kJ/mol deep when 2 $HS(AuPH_3)_2^+$ forms $[HS(AuPH_3)_2^+]_2$. Namely, when the two $HS(AuPH_3)_2^+$ form

Table 7 Bond energy ΔE_1 (in kJ/mol) decomposition of $[S(AuPH_3)_2]_2$ and ΔE_2 (in kJ/mol) decomposition of $[HS(AuPH_3)_2^+]_2$ at Xα/TZ2P level

	ΔE_1	ΔE_2
Pauli repulsion energy (E_{pauli})	761.80	205.03
Electrostatic interaction ($E_{ele.}$)	−665.11	49.64
Sum of E_{pauli} and $E_{ele.}$	96.69	254.67
Orbital interaction ($E_{orb.}$)	−221.49	−112.04
Total bonding energy ($E_{tot.}$)	−124.80	142.63

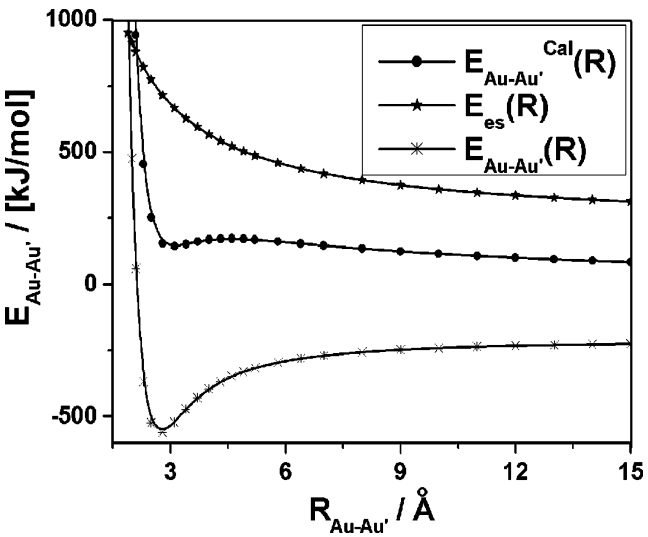

Fig. 2 Intermolecular aurophilic interaction energies ($E_{Au\text{-}Au'}$) plotted against the Au···Au′ distance of gold complexes $[HS(AuPH_3)_2^+]_2$. $E_{Au\text{-}Au'}^{cal}$ (R) represents calculated intermolecular aurophilic interaction energy. E_{es}(R) represents the coulomb energy after adding two point charges (PC). $E_{Au\text{-}Au'}$(R) represents corrected intermolecular aurophilic interaction energy

$[HS(AuPH_3)_2^+]_2$, the intermolecular aurophilic interaction is approximately 334 kJ/mol. Each Au···Au pair interaction energy is about 167 kJ/mol, and is stronger than the most aurophilic interaction systems. Schmidbaur et al. [56] studied a similar cation···cation attractive system $[O(AuPPh_3)_3^+]_2$ by adding PCs. For such a cation···cation attractive system, the number of PCs added can affect the aurophilic interaction. We acknowledge that this is a only an approximate method to calculate the intermolecular aurophilic interaction in cation···cation attractive systems.

Conclusions

In the present work, central-atom gold complexes $S(AuPH_3)_2$, $[HS(AuPH_3)_2]^+$ and their dimers were studied by means of MP2 and DFT methods. Using quantum mechanical methods, we concluded that: (1) the present geometries obtained by Xα method are in reasonable agreement with experimental values. When the top S atom obtains a H^+ proton, Au···Au distances increased. (2) The predicted structure of $[S(AuPH_3)_2]_2$ prefers a D_{2d} structure. (3) Analysis of Mulliken populations and charges show that the Au5d shell is not completely closed, and it may thus contribute to metal–metal bonding. When the monomer forms a dimer, the electronic structure changes little. (4) The HOMO–LUMO gap increases when the top S atom obtains a proton (H^+); otherwise, when two monomers formed a dimer, the chemical stability decreased. (5) Analysis of bond energy decompositions showed that for the $[S(AuPH_3)_2]_2$ molecule, the inter-molecular aurophilic interaction is −124.80 kJ/mol; for the $[HS(AuPH_3)_2^+]_2$ system, a positive BE value (no bonding) was calculated. The repulsions between the charged monomers of a dimer in the gas phase are attenuated in the solid state by the Madelung potential provided by the counterions. When 2 PCs are added to the $[HS(AuPH_3)_2^+]_2$ system, a negative binding energy is obtained.

Acknowledgments We acknowledge the financial support of the China Postdoctoral Foundation and Postdoctoral Foundation of Jiangsu Province.

References

1. Pyykkö P (1997) Chem Rev 97:597. doi:10.1021/cr940396v
2. Schmidbaur H (1990) Gold Bull 23:11
3. Zeller E, Beruda H, Schmidbaur H (1993) Inorg Chem 32:3203. doi:10.1021/ic00067a002
4. Scheraum F, Grohmann A, Huber B, Krüger C, Schmidbaur H (1988) Angew Chem Int Ed Engl 27:1544. doi:10.1002/ange.19881001130
5. Scherbaum F, Grohmann A, Müller G, Schmidbaur H (1989) Angew Chem Int Ed Engl 28:463. doi:10.1002/ange.19891010410
6. Grohmann A, Riede J, Schmidbaur H (1990) Nature 345:140. doi:10.1038/345140a0
7. Zeller E, Schmidbaur H (1993) J Chem Soc Chem Commun 69. doi:10.1039/c39930000069
8. Abel EW, Jenkins CR (1968) J Organomet Chem 14:285. doi:10.1016/S0022-328X(00)87668-8
9. Jones PG, Sheldrick GM, Hädicke E (1980) Acta Crystallogr B 36:2777. doi:10.1107/S0567740880009995
10. Schmidbaur H, Kolb A, Zeller E, Schier A, Beruda H (1993) Z Anorg Allg Chem 619:1575. doi:10.1002/zaac.19936190912
11. Canales F, Gimeno MC, Jones PG, Laguna A (1994) Angew Chem Int Ed Engl 33:769. Angew Chem 106:811. doi:10.1002/ange.19941060723
12. Schmidbaur H, Steigelmann O (1992) Z Naturf B 47:1721
13. Angermaier K, Schmidbaur H (1994) Inorg Chem 33:2069. doi:10.1021/ic00088a001
14. Rasul G, Prakash GKS, Olah GA (1997) J Am Chem Soc 119:12984. doi:10.1021/ja9729948
15. Rösch N, Görling A, Ellis DE, Schmidbaur H (1989) Angew Chem 101:1410. Angew Chem Int Ed Engl 28:1357. doi:10.1002/anie.198913571
16. Canales S, Crespo O, Gimeno MC, Jones PG, Laguna A (1999) J Chem Soc Chem Commun 679
17. Lensch C, Jones PG, Sheldrick GM (1982) Z Naturforsch Teil B 37:944
18. Schmidbaur H, Hofrelter S, Paul M (1995) Nature 377:503. doi:10.1038/377503a0
19. Canales F, Gimeno C, Laguna A, Villacampa MD (1996) Inorg Chim Acta 244:95. doi:10.1016/0020-1693(95)04759-X
20. Schmidbaur H, Gabbaï FP, Schier A, Riede J (1995) Organometallics 14:4969. doi:10.1021/om00011a001
21. Chen JH, Jiang T, Wei G, Mohamed AA, Homrighausen C, Bauer JAK, Bruce AE, Bruce MRM (1999) J Am Chem Soc 121:9225. doi:10.1021/ja991986j
22. Mohamed AA, Chen J, Bruce AE, Bruce MRM, Hill DT (2003) Inorg Chem 42:2203. doi:10.1021/ic026057z
23. Wang S, Fackler JP (1990) Inorg Chem 29:4404. doi:10.1021/ic00347a016
24. Wang SG, Schwarz WHE (2004) J Am Chem Soc 126:1266. doi:10.1021/ja035097e
25. Fang H, Wang SG (2006) J Mol Struct THEOCHEM 773:15. doi:10.1016/j.theochem.2006.06.034
26. Fang H, Wang SG (2007) J Phys Chem A 111:1562. doi:10.1021/jp064656b
27. Fang H, Wang SG (2007) J Mol Model 13:255. doi:10.1007/s00894-006-0156-5
28. Sladek A, Angermaier K, Schmidbaur H (1996) J Chem Soc Chem Commun 1959:1
29. Häberlen OD, Rösch N (1993) J Phys Chem 97:4970. doi:10.1021/j100121a019
30. Frisch MJ, Trucks GW, Schlegel HB, Scuseria GE, Robb MA, Cheeseman JR, Zakrzewski VG Montgomery JAJr., Stratmann RE, Burant JC, Dapprich S, Millam JM, Daniels AD, Kudin KN, Strain MC, Farkas O, Tomasi J, Barone V, Cossi M, Cammi R, Mennucci B, Pomelli C, Adamo C, Clifford S, Ochterski J, Petersson GA, Ayala PY, Cui Q, Morokuma K, Malick DK, Rabuck AD, Raghavachari K, Foresman JB, Cioslowski J, Ortiz JV, Stefanov BB, Liu G, Liashenko A, Piskorz P, Komaromi I, Gomperts R, Martin RL, Fox DJ, Keith T, Al-Laham MA, Peng CY, Nanayakkara A, Gonzalez C, Challacombe M, Gill PMW, Johnson B, Chen W, Wong MW, Andres JL, Gonzalez C, Head-Gordon M, Replogle ES, Pople JA (1998) Gaussian 98, revs. A9 and A11.3, Gaussian Inc.,Pittsburgh, PA
31. Te Velde G, Bichelhaupt FM, Baerends EJ, Fonseca Guerra C, Van Gisbergen SJA, Snijders JG, Ziegler T (2001) J Comput Chem 22:931. doi:10.1002/jcc.1056

32. Slater JC (1951) Phys Rev 81:385. doi:10.1103/PhysRev.81.385
33. Slater JC (1974) Quantum theory of molecules and solids, vol 4. McGraw-Hill, New York
34. Gaspar R (1954) Acta Phys 3:263
35. Schwarz K (1972) Phys Rev B 5:2466. doi:10.1103/PhysRevB.5.2466
36. Vosko SH, Wilk L, Nusair M (1980) Can J Phys 58:1200
37. Becke AD (1988) J Chem Phys 88:2547. doi:10.1063/1.454033
38. Perdew JP (1986) Phys Rev B 34:406
39. Perdew JP (1992) Phys Rev B 46:6671. doi:10.1103/PhysRevB.46.6671
40. Te Velde G, Baerends EJ (1992) J Comput Phys 99:84. doi:10.1016/0021-9991(92)90277-6
41. Van Lenthe E, Ehlers AE, Baerends EJ (1999) J Chem Phys 110:8943. doi:10.1063/1.478813
42. Van Lenthe E, Baerends EJ, Snijders JG (1994) J Chem Phys 101:9783. doi:10.1063/1.467943
43. Van Lenthe E, Snijders JG, Baerends EJ (1996) J Chem Phys 105:6505. doi:10.1063/1.472460
44. Van Lenthe E (1996) Int J Quantum Chem 57:281. doi:10.1002/(SICI)1097-461X(1996)57:3<281::AID-QUA2>3.0.CO;2-U
45. Andrae D, Haussermann U, Dolg M, Stoll H, Preuss H (1990) Theor Chim Acta Berl 77:123. doi:10.1007/BF01114537
46. Pyykkö P, Runeberg N, Mendizabal F (1997) Chem Eur J 3:1451. doi:10.1002/chem.19970030911
47. Pyykkö P, Tamm T (1998) Organometallics 17:4842. doi:10.1021/om980255+
48. Riedel S, Pyykkö P, Mata RA, Werner HJ (2005) Chem Phys Lett 405:148. doi:10.1016/j.cplett.2005.02.013
49. Krüger S, Stener M, Mayer M, Nörtemann F, Rösch N (2000) J Mol Struct 527:63
50. Sladek A, Schneider W, Angermaier K, Bauer A, Schmidbaur H (1996) Z Naturforsch [B] 517:65
51. Sladek A, Schmidbaur H (1995) Chem Ber 128:907. doi:10.1002/cber.19951280909
52. Armin H, Mitzel NW, Schmidbaur H (2001) J Am Chem Soc 123:5106. doi:10.1021/ja010398e
53. Ziegler T (1984) J Am Chem Soc 106:5901. doi:10.1021/ja00332a025
54. Ziegler T, Rauk A (1977) Theor Chim Acta 46:1
55. Famiglietti C, Baerends EJ (1981) Chem Phys 62:407. doi:10.1016/0301-0104(81)85135-X
56. Chung SC, Krüer S, Schmidbaur H, Rösch N (1996) Inorg Chem 35:5387. doi:10.1021/ic960418r